



Submitted to

14th International Workshop on Deep Inelastic Scattering, DIS2006, April 20-24, 2006, Tsukuba, Japan

www-h1.desy.de/h1/www/publications/conf/conf_list.html

H1prelim-06-011

Threejet production in deep inelastic e - p scattering and low- x parton dynamics at HERA

H1 Collaboration

Abstract

Differential threejet cross sections in deep inelastic scattering processes at low x and Q^2 have been measured with the H1 detector using an integrated luminosity of 44.2 pb^{-1} . Threejet events are identified using the inclusive k_{\perp} cluster algorithm in the γ^*p rest frame. The cross sections are given at the level of parton jets and correspond to the kinematic range $10^{-4} < x < 10^{-2}$, $5 \text{ GeV}^2 < Q^2 < 80 \text{ GeV}^2$, $E_{\perp, \text{jet}}^* > 4 \text{ GeV}$ and $-1 < \eta_{\text{jet}} < 2.5$. Three phase-space regions have been selected in order to study parton dynamics from the most global to the most restrictive regions of forward going (close to the proton-direction) jets. The measurements of threejet cross sections are compared with fixed order QCD predictions of $\mathcal{O}(\alpha_s^2)$ and $\mathcal{O}(\alpha_s^3)$ and with two leading order MC predictions where additional partons are generated by initial state radiation and by the color dipole model respectively. A good description is given by the $\mathcal{O}(\alpha_s^3)$ prediction for which remaining differences are concentrated at low x and topologies with two forward jets, which are most sensitive to unordered gluon radiation. The LO MC with unordered gluon radiation modeled by the color dipole model gives a good overall description of the data. We interpret these results as strong hints for the presence of large contributions from non- k_{\perp} -ordered gluon radiation needed to describe threejet production at low x and forward rapidities.

1 Introduction

The study of parton dynamics at low x has been an active area of research since early HERA operation because HERA has entered a new kinematic regime where the approximations of the DGLAP evolution equations may no longer be valid. These approximations neglect terms proportional to $\alpha_s \cdot \ln(1/x)$ which are naturally expected to become large at small x . These effects are best studied in the hadronic final state since these terms may, compared to DGLAP, lead to a significant enhancement of gluon radiation unordered in transverse momentum. This effect should be largest for high P_\perp forward jets (near to the proton direction). Various measurements [1]–[2] have shown, that the rate of forward jets is indeed higher than predicted by LO QCD predictions including initial state radiation. However, predictions including a resolved photon contribution or unordered gluon radiation as implemented in the color dipole model were shown to give a decent description of forward jet data and of dijet cross sections at low x . Measurements of the ZEUS collaboration [3] have shown that the description of inclusive forward jet production is significantly improved by up to a factor 10 by the fixed order α_s^2 compared to the order α_s prediction. This paper concentrates on threejet events which require at least one radiated gluon in addition to the two hard scattered partons and the comparison with fixed order QCD predictions which for threejet events are either LO or NLO. In addition two LO Monte Carlo generators which were able to describe forward jet and dijet production at low x are also tested. These are the generator RAPGAP with initial state radiation including a resolved photon contribution and DJANGO which uses the color dipole model to produce additional gluon radiation.

2 Kinematics

Figure 1 shows two of the hard DIS processes dominating at low x , which lead to three or more jets in the final state. The diagrams correspond to order α_s^2 and α_s^3 contributions to the cross section. The radiated gluons are predominantly emitted into the forward direction whereas the quarks from the hard scattering process are mostly central.

The relevant kinematic variables used are the Bjørken variable $x = Q^2/Q_{\max}^2$ and Q^2 , the momentum transfer squared. Jets are selected using the inclusive k_\perp algorithm in the γ^*p center of mass system. They will be characterised by their transverse momentum P_\perp^{*1} and their pseudorapidity η in the laboratory system. The 3-jet topology is fully described by the variables defined in [4]. We use only a subset of these variables namely the normalised energy of the jets $X_i = E'_i / \sum_j E'_j$ and the two angles θ' and ψ' as defined in figure 2. These observables are measured in the 3-jet center of mass frame.

3 Monte Carlo Simulations and Fixed Power QCD Predictions

In the analysis two Monte Carlo programs were used to correct the data for detector inefficiencies and migrations, and to compare the measured cross sections with model predictions. Both

¹Observables in the γ^*p center of mass frame carry a *.

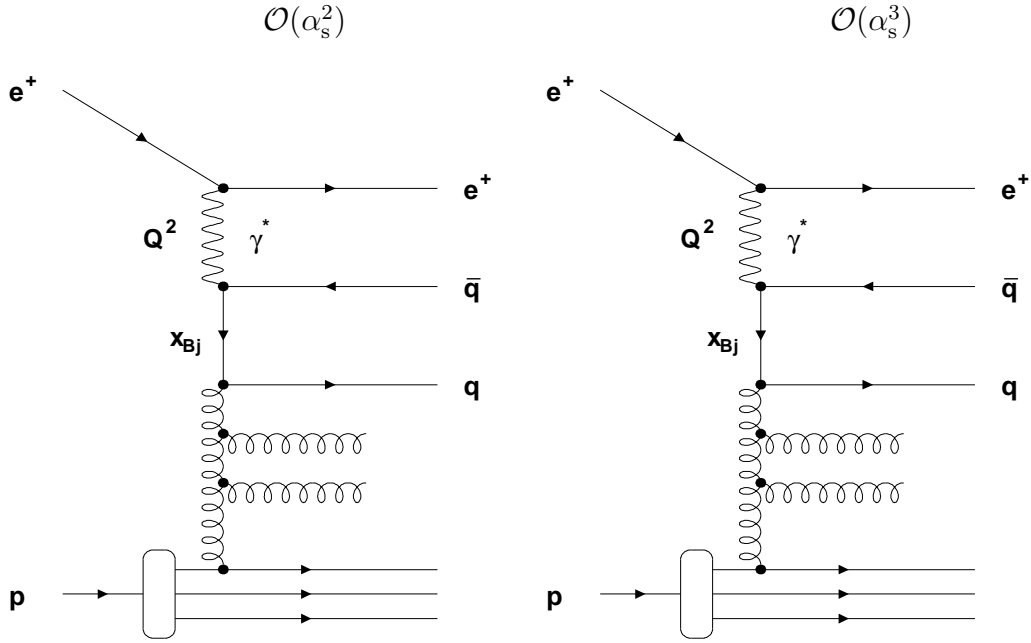


Figure 1: Leading and next to leading order diagrams to 3-jet production in DIS at HERA with one and two radiated gluons, respectively.

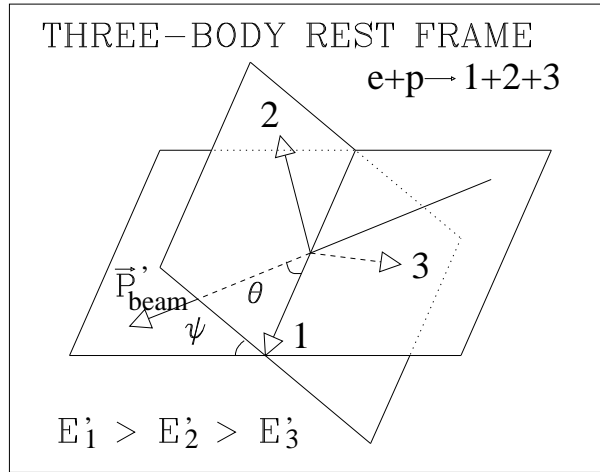


Figure 2: Definition of the angles θ' and ψ' in the threejet rest system. The figure was taken from [4]

use leading order matrix elements for the hard QCD $2 \rightarrow 2$ subprocess which are convoluted with parton distributions of the proton and the photon, taken at the scale $\mu^2 = Q^2$ (DJANGO) and $\mu^2 = Q^2 + \hat{p}_\perp^2$ (RAPGAP), respectively, where \hat{p}_\perp is the transverse momentum of the emerging hard partons. The RAPGAP 2.08 Monte Carlo program [5] adds a resolved photon component for which the SaS 2D parton distribution functions are used, which were found to give a

good description of the effective photon structure function as measured by H1. Higher order effects are simulated using parton showers in the leading $\log(\mu)$ approximation (MEPS), and the Lund string model is used for hadronisation. The DJANGO [6] Monte Carlo program on the other hand uses the color dipole model (CDM) [7] which creates additional gluon radiation not ordered in k_{\perp} . Again the Lund string fragmentation is used for hadronisation. Radiative corrections are applied using the HERACLES program.

Fixed order QCD predictions at parton level are calculated using the NLOjet++ program [8] which is able to predict threejet parton cross sections in leading (LO) and next to leading (NLO) order.

4 Experimental Procedure

4.1 H1 Detector

A detailed description of the H1 detector can be found in [9]. Here, a brief account of the components most relevant to the present analysis is given. The H1 coordinate system convention defines the outgoing proton beam direction as the positive z axis and the polar scattering angle θ such that the pseudorapidity $\eta = -\ln \tan(\theta/2)$ increases along z .

The hadronic final state X is measured with a tracking and a calorimeter system. The central ep interaction region is surrounded by two large concentric drift chambers, located inside a 1.15 T solenoidal magnetic field. Charged particle momenta are measured in the range $-1.5 < \eta < 1.5$ with a resolution of $\sigma/p_T = 0.01 p_T/\text{GeV}$. A finely segmented electromagnetic and hadronic liquid argon calorimeter (LAr) covers the range $-1.5 < \eta < 3.4$. The energy resolution is $\sigma/E = 0.11/\sqrt{E/\text{GeV}}$ for electromagnetic showers and $\sigma/E = 0.50/\sqrt{E/\text{GeV}}$ for hadrons, as measured in test beams. A lead/scintillating fibre calorimeter (SPACAL) covers the backward region $-4 < \eta < -1.4$. It is used to detect the scattered positron.

4.2 Event Selection

The data used in this analysis were taken in the 1999 and 2000 running periods, in which HERA collided 920 GeV protons with 27.5 GeV positrons. The data are collected using a trigger which requires the scattered electron to be measured in the electron detector and at least one high transverse momentum track ($p_{\perp} > 800$ MeV) in the central jet chamber. The scattered positron is required to be measured in the backward electromagnetic calorimeter with an energy $E'_e > 9$ GeV. The kinematic range is chosen to be $5 \text{ GeV}^2 < Q^2 < 80 \text{ GeV}^2$ and $0.1 < y < 0.7$.

Jets are formed from the tracks and clusters of the hadronic final state, using the inclusive k_{\perp} cluster algorithm (with a distance parameter of 1.0) in the γ^*p rest frame. At least 3 jets are required, with transverse energies $E_{\perp}^* > 4$ GeV for all jets and $E_{\perp 1}^* + E_{\perp 2}^* > 9$ GeV for the sum of the leading and subleading jet, respectively. The jet axes are required to lie within the region $-1 < \eta_{\text{jet}} < 2.5$, well within the acceptance of the LAr calorimeter except for one jet which is required to be central e.g. in the range $-1 < \eta_{\text{jet}} < 1.3$ in order to guarantee a good trigger efficiency. After all cuts we are left with 38400 events with at least three jets of which 6000 have more than 3 jets. This is a very large statistical improvement compared to earlier studies.

Cross Section Definition

$0.1 < y < 0.7$ $4 \text{ GeV}^2 < Q^2 < 80 \text{ GeV}^2$
$N_{\text{jet}} \geq 3$ $E_{\perp, \text{jet}}^* > 4 \text{ GeV}$ $E_{\perp, \text{jet1}}^* + E_{\perp, \text{jet2}}^* > 9 \text{ GeV}$ $-1 < \eta_{\text{jet}}^{\text{lab}} < 2.5$
one jet in the range $-1 < \eta_{\text{jet}}^{\text{lab}} < 1.3$

Table 1: The kinematic domain in which the cross sections are measured. The jets are reconstructed using the inclusive k_{\perp} algorithm with the distance parameter set to 1.0 for detector jets as well as for the jets on parton or hadron level

4.3 Kinematic Reconstruction

The energy E'_e of the scattered electron is measured directly in the backward electromagnetic calorimeter and the inelasticity y is derived from it

$$y = 1 - \frac{E'_e}{E_e} \sin^2 \frac{\theta'_e}{2}$$

where E_e is the electron beam energy. The virtuality of the exchanged virtual Boson and the Björken scaling variable is reconstructed from

$$Q^2 = 4E_e E'_e \cos^2 \frac{\theta'_e}{2}, \quad x = \frac{Q^2}{ys},$$

where θ'_e is the angle of the scattered positron and s is the ep center of mass energy squared.

The hadronic system X , containing the jets, is measured in the LAr and SPACAL calorimeters and the central tracking system. Calorimeter cluster energies and track momenta are combined using algorithms which avoid double counting.

4.4 Cross Section Measurement

The measured cross sections are defined at the level of parton jets for comparisons with fixed order QCD predictions and at the level of stable hadrons for the comparison with LO Monte Carlo generators. The data are corrected in two steps. The first step corrects from detector jets to jets at stable hadron level accounting for detector inefficiencies and migrations of kinematic quantities in the reconstruction (detector correction). The second step corrects for the effects of hadronisation from hadron jets to parton jets ('inverse' hadronisation correction). Since the two steps are logically independent, the uncertainties of both correction factors are added in quadrature to determine the uncertainty of the cross sections at the parton jet level. The correction factors for both steps are determined using the DJANGO Monte Carlo program which offers a

better description of the parton distributions than RAPGAP which is therefore only used for the estimation of systematic effects. For generated events, the H1 detector response is simulated in detail and the Monte Carlo events are subjected to the same analysis chain as the data. A reliable determination of the correction factors requires a good description of both the kinematic distributions and the energy flow in the events. Since both generators show significant deviations from the data distributions, the events are weighted in a few variables to adjust their kinematic distributions to the data. These variables are the P_{\perp} of the leading jet, $\eta_1 - \eta_2$, $\eta_1 + \eta_2$ and Q^2 . The weighted simulations give a reasonable description of the shapes of all data distributions. According to the simulations, the detector level observables are well correlated with the hadron and parton level quantities. Remaining differences are considered in the estimate of the systematic uncertainties of the correction factors.

The kinematic region for which the cross sections are measured is given in table 1. An analysis of systematic uncertainties has been performed in which the sensitivity of the measurement to variations of the detector calibration and the Monte Carlo Models used for correction are evaluated. The dominant systematic error on the cross sections arises from the uncertainty in the LAr calorimeter energy scale and from the uncertainty of the corrections needed to go from detector to hadron jets and from hadron to parton jets. The latter has been estimated by using RAPGAP in addition to DJANGO to determine the cross sections and using 50 % of the difference of the correction factors evaluated by the two generators as estimate of their systematic error. All cross sections have an absolute normalisation error of 18% which is normally not shown.

5 Results

In Figures 3 to 5, the differential cross sections are presented for events with 3 or more jets for the number of jets (N_{jet}), x , the pseudorapidities of the three jets and the 3-jet variables describing relative jet energy and angles. The kinematic range for which the cross sections are determined is specified in table 1. The figures also show the predictions of the NLO++ fixed order QCD prediction in LO (dashed-dotted histogram) and NLO (solid line and shaded error bands). The error bands of the NLO predictions are scale errors obtained by varying the renormalisation and factorisation scale μ in the QCD prediction by a factor 2 and 0.5, respectively. The value of $\alpha_s(m_{Z^0})$ has been fixed to 0.118 and the parton parametrisation CTEQ6 has been used. Figure 3 shows the jet multiplicity distribution which extends up to $N_{\text{jet}} = 7$. For this distributions also the predictions of the two LO Monte Carlo programs are shown. It can be noted that the color dipole model (DJANGO + CDM) gives an excellent description of this distribution while RAPGAP fails. The NLO prediction agrees for $N_{\text{jet}} = 3$, misses a fraction of 4-jet events and of course does not produce any events with more than 4 jets. In total it misses 18% of events with four or more jets.

The kinematic distributions shown in figures 3–5 are not described by the LO ($\mathcal{O}(\alpha_s^2)$) QCD predictions neither in shape nor in magnitude. Main discrepancies are seen at low x and for forward jets (large η) where by far too few events are predicted. The NLO prediction improves the situation dramatically in all regions where deviations are observed. At lowest x the discrepancy

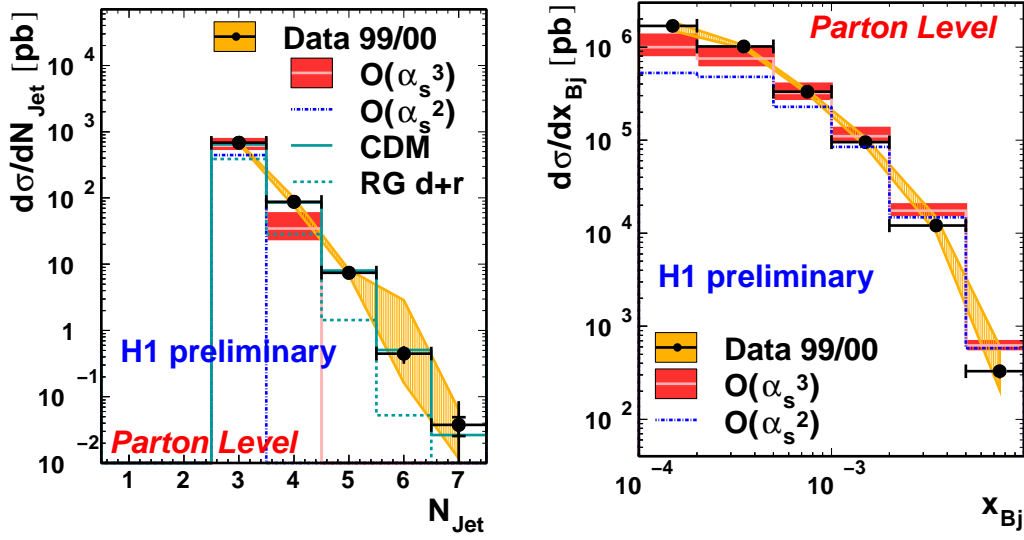


Figure 3: Differential cross sections in the number of jets N_{jet} and the Bjørken scaling variable x . The inner error bars represent the statistical error of the data, the total error bars correspond to the statistical and uncorrelated systematic errors added in quadrature. The (orange) hatched error bands show the estimate of the correlated systematic uncertainties. The data has an additional overall normalisation error of 19 %. The shaded (red) band shows the NLO prediction where the size of the band indicates the scale uncertainty of the NLO calculation, the dashed dotted line represents the LO prediction. The data for N_{jet} are also compared to the two LO Monte Carlo programs RAPGAP (dotted line) and DJANGO (CDM) (solid line).

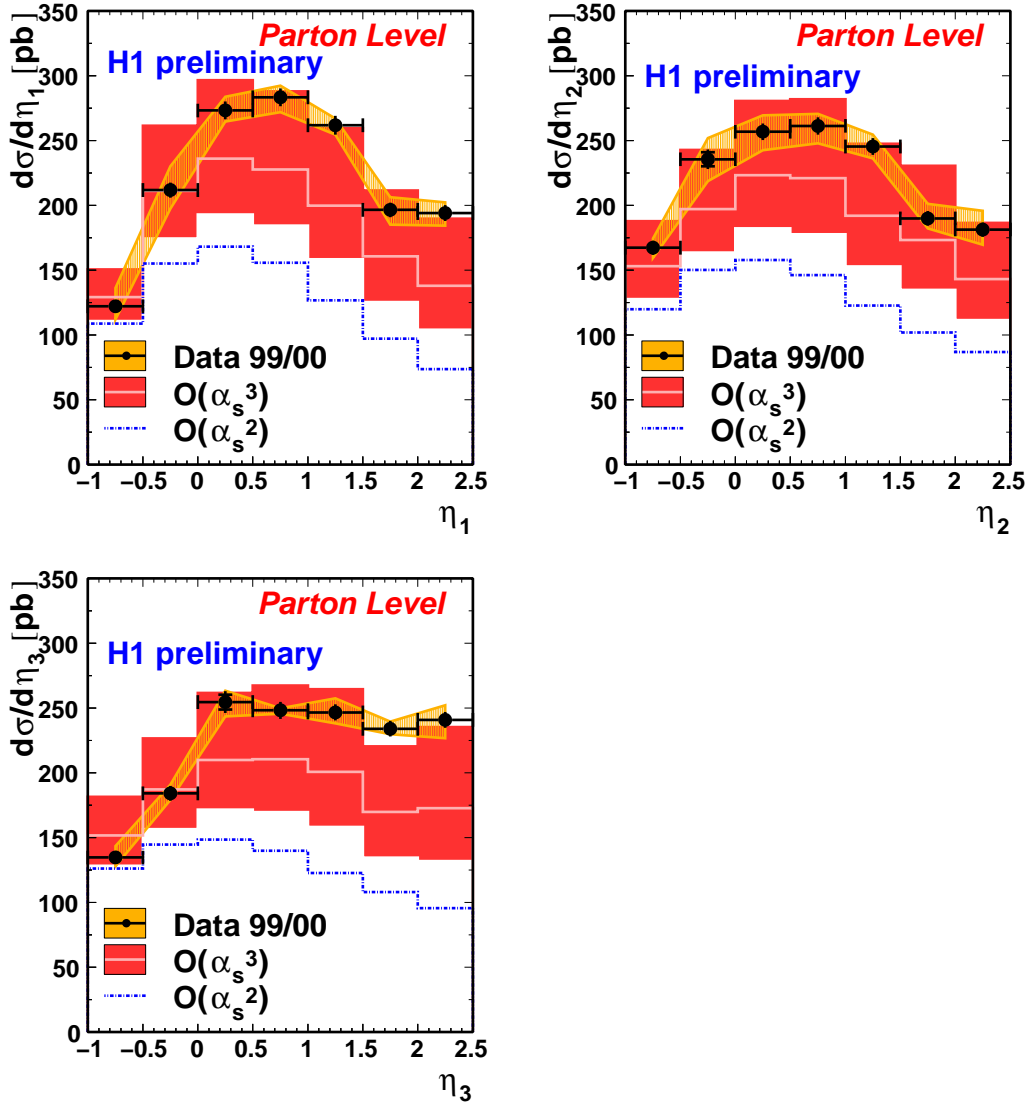


Figure 4: Differential cross sections in the pseudorapidity η_i for each of the three jets ($P_{\perp 1}^* > P_{\perp 2}^* > P_{\perp 3}^*$) compared to the LO (dashed-dotted line) and to the NLO (shaded (red) error band) prediction. Other details are as in the caption to fig. 3

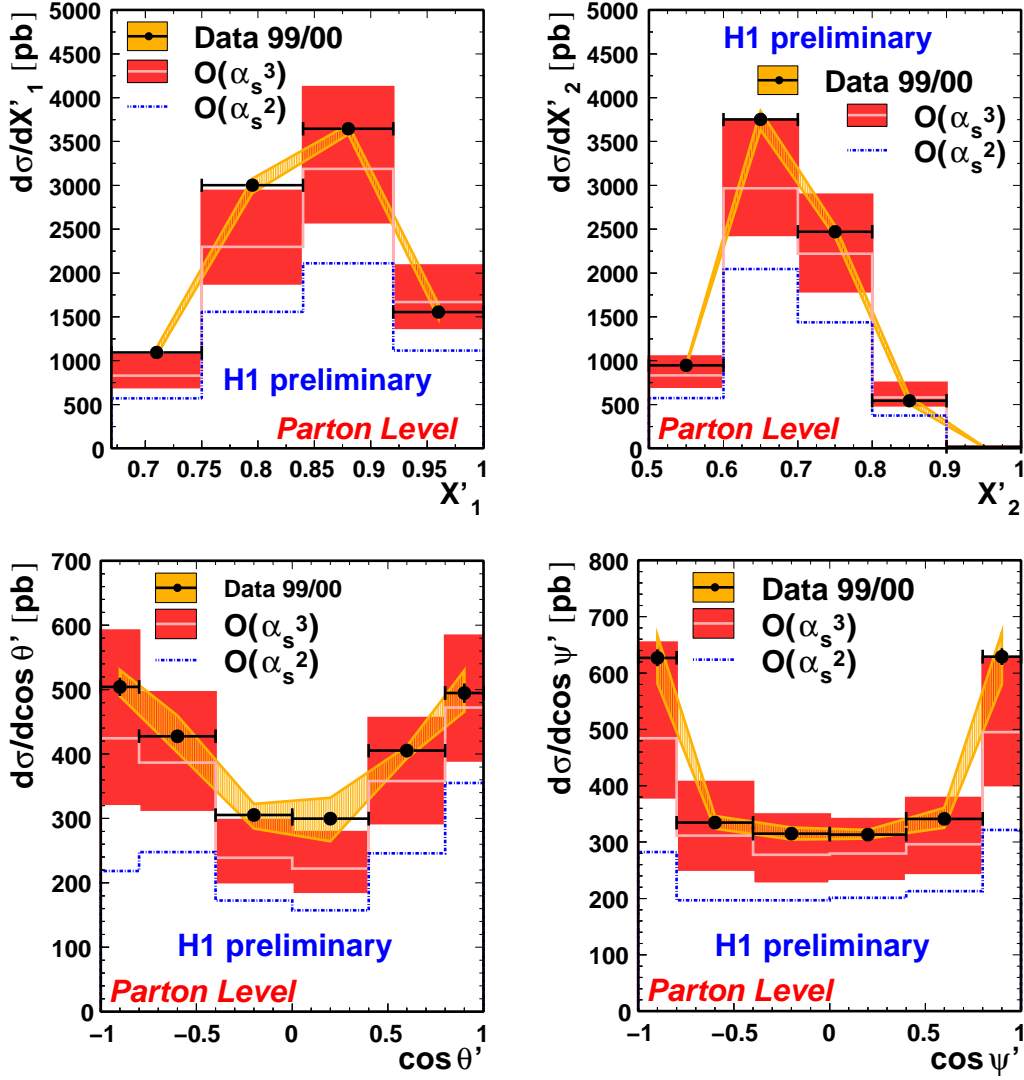


Figure 5: Differential cross sections of the normalised energies X'_i of the two leading jets ($E'_1 > E'_2 > E'_3$ in the 3-jet center of mass frame) and the two angles θ' and ψ' as defined in figure 2 compared to the LO and the NLO prediction. Other details are as in the caption to fig. 3

diminishes from a factor of about 3.3 to 1.7. The threejet variables of figure 5 are well described by the NLO prediction apart from an 18 % difference in normalisation. The conclusion is therefore that events with more than 3 jets are missing mainly at low x and large η .

5.1 Forward Jet Selections

Here we look at a restricted sample of events with forward jets where the observed differences for the global selection were largest and where the largest sensitivity to unordered gluon radiation is expected. A forward jet is defined in agreement with earlier publications [2] by

$$\theta_{\text{jet}} < 20^\circ \text{ and } x_{\text{jet}} = \frac{E_{\text{jet}}^*}{E_{p, \text{beam}}} > 0.035$$

The forward jet sample is further divided into two subsamples. Sample 1 requires two central jets in the range $-1 < \eta_{\text{jet}} < 1$ and one forward jet, sample 2 requires one central jet and two forward jets (one forward jet and one additional jet with $\eta > 1$). It is expected that forward jets are predominantly produced by gluon radiation while central jets should predominantly originate from the hard scattering process. This is confirmed by a study of the parton composition

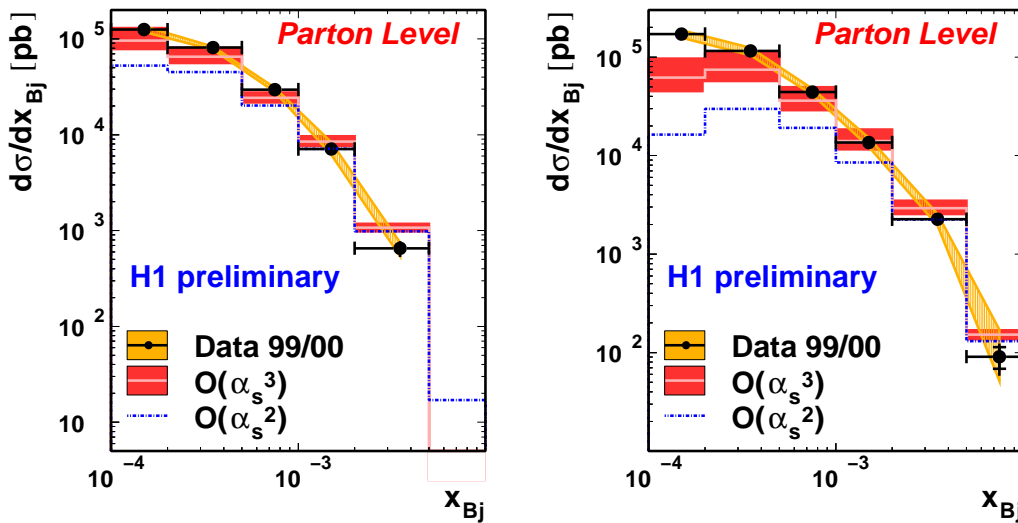


Figure 6: Differential cross sections in the Bjørken scaling variable x for the samples with two central (left) and with two forward jets (right). Other details are as in the caption to fig. 3

of threejet events using the DJANGO (CDM) Monte Carlo program. Therefore sample 1 will have many events with only one gluon radiation while sample 2 with two forward jets will have a larger fraction of events with two radiated gluons thus being more sensitive to unordered gluon radiation. Results are shown in figures 6 and 7 for the variables x , η_1 and $P_{\perp 1}^*$. The fixed order NLO prediction gives a rather good description for the sample with two central jets, where the step from LO to NLO improves the agreement at low x and large rapidity dramatically by more than a factor 2, missing only about 30% of events. The sample with two forward jets on the other hand gives an even more dramatic change reducing the discrepancy at small x from a factor of 10 to 3.5 when going from the LO to the NLO prediction, but a large discrepancy remains. In

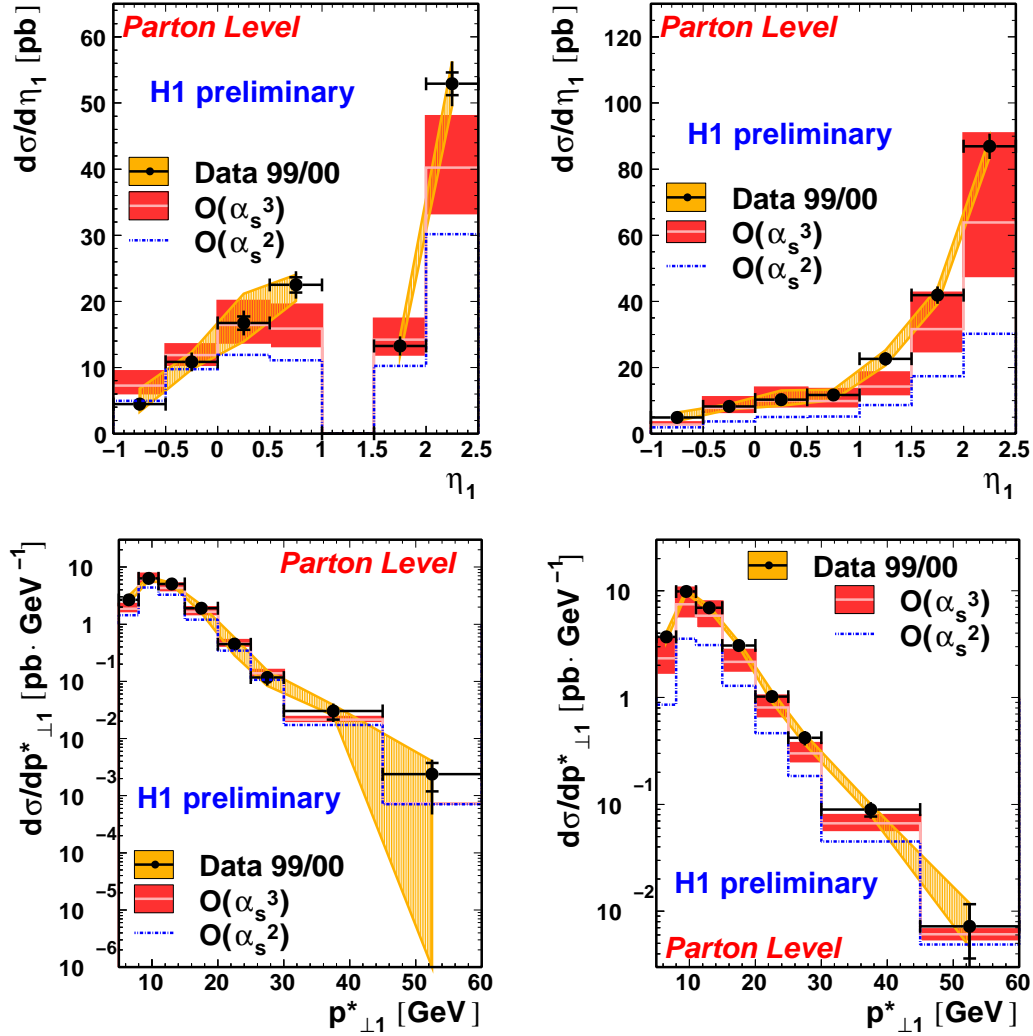


Figure 7: Differential cross sections of the pseudorapidity (top) and of the transverse momentum (bottom) of the leading jet for the samples with two central (left) resp. two forward jets (right). Other details are as in the caption to fig. 3

summary the main discrepancies between data and the fixed order NLO prediction are found at small x and large rapidities for the sample with two forward jets. This is exactly the kinematic region where unordered gluon radiation is expected to make a large contribution. It should be noted that the DGLAP evolution equation in order α_s^3 include additional terms $\propto \alpha_s \cdot \ln(1/x)$ not present in leading order.

6 Comparison to the LO Monte Carlo Programs

In a last step we compare to the two LO Monte Carlo Programs RAPGAP (with resolved photon contribution) and DJANGO (with color dipole model) which have both been successful in describing the forward jet data and the dijet cross sections to the measured cross sections at hadron jet level, especially to the angular distributions of the the threejet system. Here the comparison is made to the non-weighted predictions of the MC generators. Figures 8 and

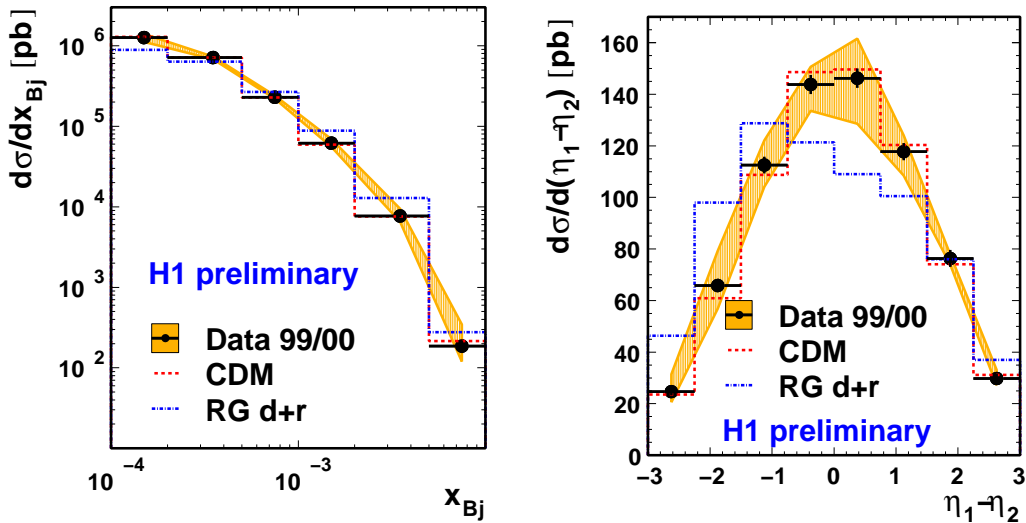


Figure 8: Differential cross sections at hadron jet level in the Bjørken scaling variable x and the difference of the pseudorapidities of the two leading jets. The inner error bars represent the statistical error of the data, the total error bars correspond to the statistical and uncorrelated systematic errors added in quadrature. The correlated systematic errors are shown by the hatched error band. The data are compared to the two LO Monte Carlo programs DJANGO (CDM) (dashed line) and RAPGAP (dashed dotted line). Both Monte Carlo cross sections are scaled to the data cross sections by factors of 1.08 (DJANGO) resp. 1.74 (RAPGAP)

9 show the comparison for the threejet cross sections in the Bjørken scaling variable x , the difference of the pseudorapidity of the two leading P_{\perp}^* jets ($\eta_1 - \eta_2$), the variables X_1 , X_2 and the two threejet angles $\cos \theta'$ and $\cos \psi$. Figure 10 shows the two angles for the 2 forward jet sample compared to the LO MC predictions at hadron jet level and also the parton jet level cross sections compared to the fixed order NLO++ QCD predictions. Since the absolute normalisation of the RAPGAP and DJANGO predictions are too low by 74% and 8% respectively, the Monte Carlo predictions are scaled up to the data in order to compare only the shape of the distributions. The

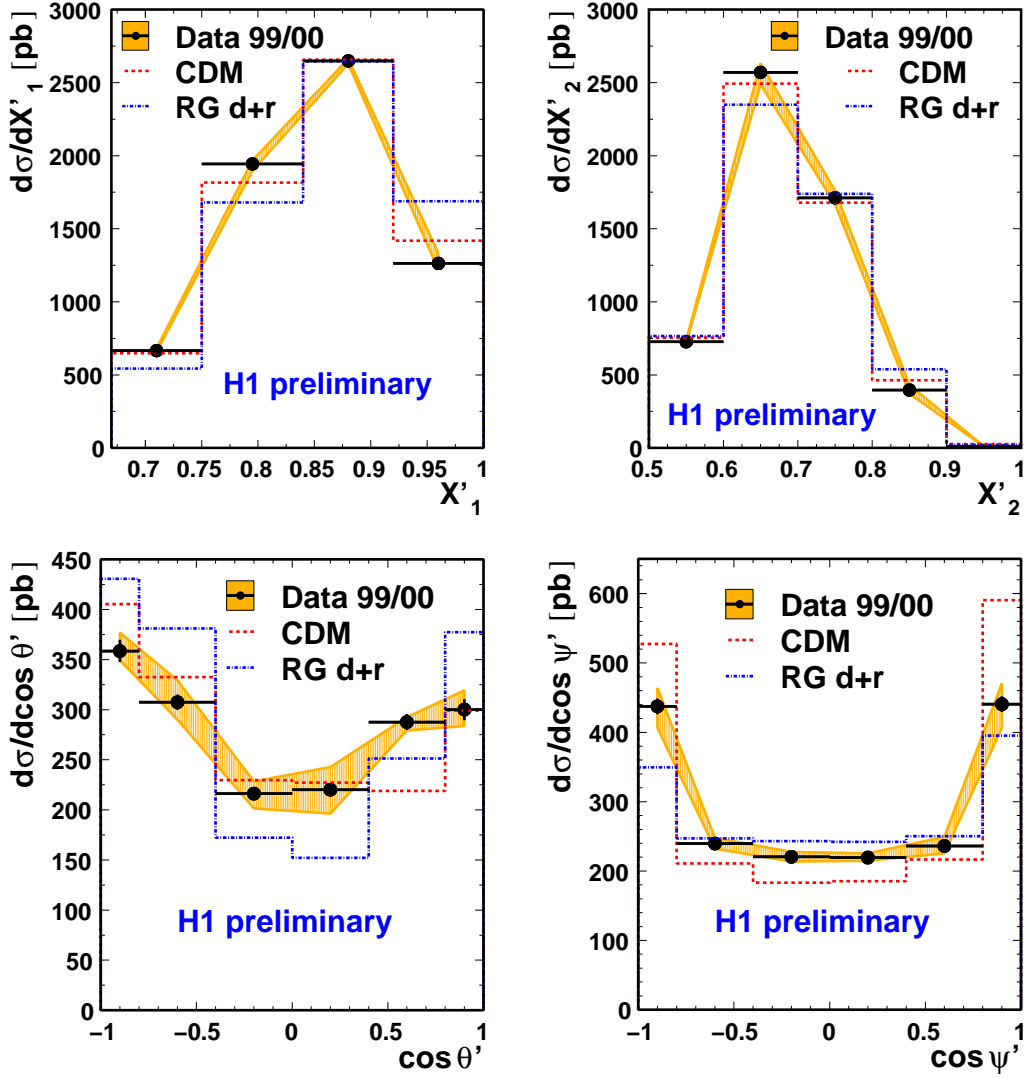


Figure 9: Differential cross sections of the normalised energies $X'_i = \frac{E'_i}{E'_1 + E'_2 + E'_3}$ of the two leading jets ($E'_1 > E'_2 > E'_3$) in the 3-jet center of mass frame and the two angles θ' and ψ' as defined in figure 2 at hadron jet level compared to the two LO Monte Carlo programs. Other details are as in the caption to fig. 8

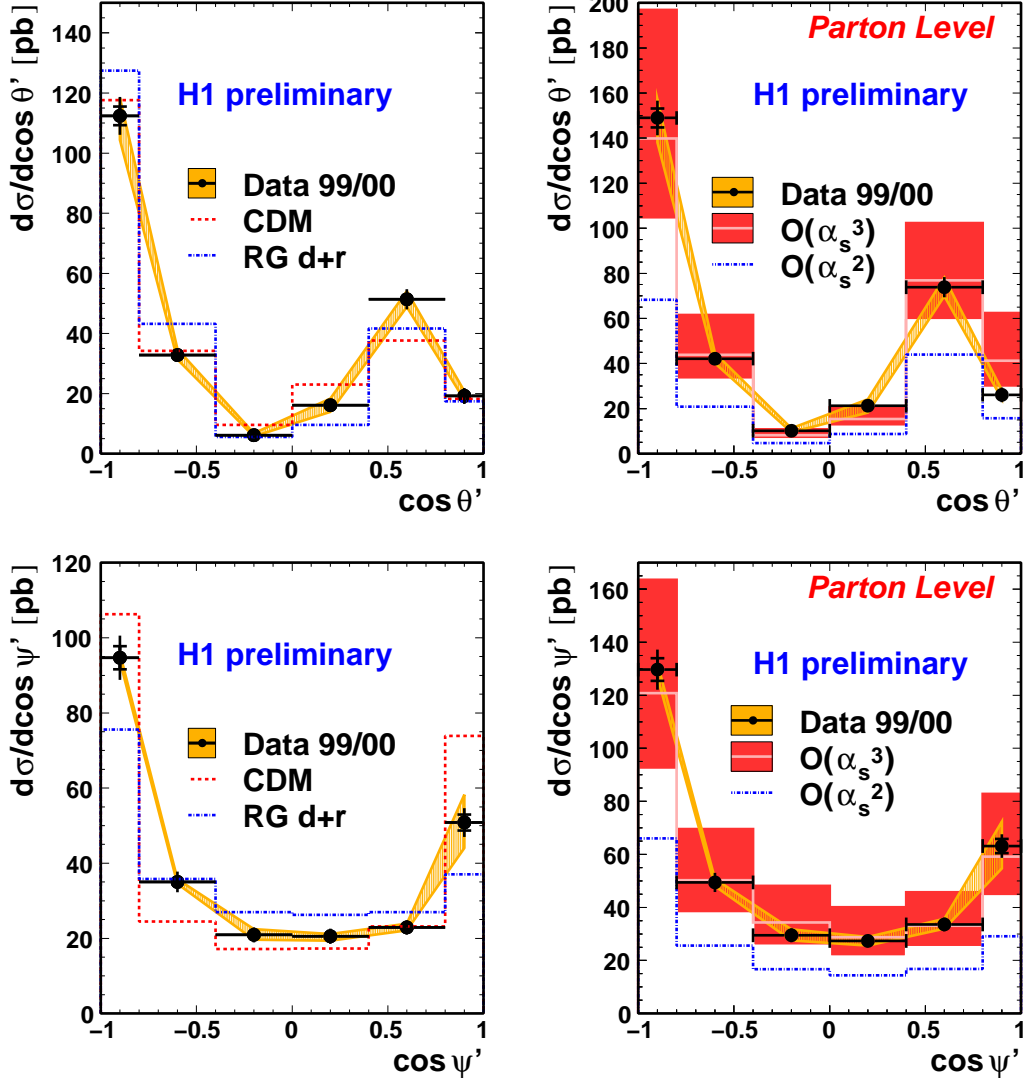


Figure 10: Differential cross sections in the two angles as introduced in figure 2 for the sample with two forward jets. Top: $\cos \theta'$, bottom: $\cos \psi'$. On the left side, the data are compared to both LO Monte Carlo programs (for details see caption to figure 8), on the right side the parton jet level cross sections are compared to the LO and NLO prediction (details see figure 3), normalised to the data cross section by applying a factor of 1.34 to both the LO and the NLO prediction

same is done for the NLO comparison. RAPGAP fails to describe the data. DJANGO+CDM on the other hand compares remarkably well. It starts to fail however in describing the threejet angles where especially for the 2 forward jet sample the NLO prediction is significantly better.

7 Summary

In contrast to inclusive and dijet jet studies, threejet events in DIS require at least the radiation of one hard gluon in addition to the two partons from the dominating hard gluon-fusion scattering process. They are therefore ideally suited to study gluon radiation at low x and to search for unordered radiation since kinematic regimes can be selected which lead to a good separation of partons from the hard scattering process and the radiated hard gluons. As known since a long time from various dijet and inclusive forward jet measurements, the data show a large excess of forward jets at low x compared to LO DGLAP predictions. Such an excess is also seen in this analysis of threejet events. However, this excess can neither be explained by additional k_{\perp} ordered initial state radiation nor by the addition of a resolved photon contribution which still worked for inclusive forward jets and dijets. The addition of non k_{\perp} -ordered gluon radiation as implemented in the color dipole model (CDM) on the other hand gives a remarkably good description of the threejet events and even of higher multiplicities. The most remarkable result of the present analysis however is the success of the fixed order QCD prediction in order α_s^3 . The addition of diagrams which allow two gluons to be radiated improves the agreement between data and the prediction dramatically and closes most of the gap between the measured cross sections and the LO ($\mathcal{O}(\alpha_s^2)$) prediction, especially for the kinematic selection with two central and one forward jet. The NLO prediction is especially good in describing the relative angles of the threejet topology where it is significantly better than the description by the color dipole model. Remaining discrepancies are concentrated at x values below 10^{-3} and events where two jets are going forward. This is a topology which is most sensitive to gluon radiation because the two forward jets are predominantly due to two radiated gluons. We conclude therefore that unordered gluon emission plays a significant role at low x . It is important to note that the NLO prediction includes for the first time also additional terms $\propto \alpha_s \cdot \ln(1/x)$, which lead to unordered gluon emission over the full phase space.

Acknowledgements

We are grateful to the HERA machine group whose outstanding efforts have made and continue to make this experiment possible. We thank the engineers and technicians for their work in constructing and now maintaining the H1 detector, our funding agencies for financial support, the DESY technical staff for continual assistance, and the DESY directorate for the hospitality which they extend to the non DESY members of the collaboration. We thank J. Bartels for useful discussions.

References

- [1] J. Breitweg *et al.* [ZEUS Collaboration], *Measurement of dijet production in neutral current deep inelastic scattering at high Q^2 and determination of α_s* , Phys. Lett. B **507** (2001) 70 [arXiv:hep-ex/0102042],
A. Aktas *et al.* [H1 Collaboration], *Inclusive dijet production at low Björken- x in deep inelastic scattering*, Eur. Phys. J. C **33** (2004) 477 [arXiv:hep-ex/0310019],
A. Aktas *et al.* [H1 Collaboration], *Measurement of dijet production at low Q^2 at HERA*, Eur. Phys. J. C **37** (2004) 141 [arXiv:hep-ex/0401010].
- [2] A. Aktas *et al.* [H1 Collaboration], *Forward jet production in deep inelastic scattering at HERA*, arXiv:hep-ex/0508055.
- [3] S. Chekanov *et al.* [ZEUS Collaboration], *Forward jet production in deep inelastic $e p$ scattering and low- x parton dynamics at HERA*, arXiv:hep-ex/0502029.
- [4] S. Geer, T. Asakawa, *The Analysis of Multijet Events Produced at High Energy Hadron Colliders*, Phys. Rev. D **53** (1996) 4793 [arXiv:hep-ph/9510351].
- [5] H. Jung, *Hard diffractive scattering in high-energy $e p$ collisions and the Monte Carlo generation RAPGAP*, Comput. Phys. Commun. **86** (1995) 147.
- [6] K. Charchula, G. A. Schuler, H. Spiesberger, *Combined QED and QCD radiative effects in deep inelastic lepton - proton scattering: The Monte Carlo generator DJANGO6*, Comput. Phys. Commun. **81** (1994) 381; <http://wwwthep.physik.uni-mainz.de/hspiesb/djangoh/djangoh.html>.
- [7] Y. I. Azimov, Y. L. Dokshitzer, V. A. Khoze, S. I. Troian, *The String Effect and QCD Coherence*, Phys. Lett. B **165** (1985) 147;
G. Gustafson, *Dual Description of a Confined Color Field*, Phys. Lett. B **175** (1986) 453;
G. Gustafson, U. Pettersson, *Dipole Formulation of QCD Cascades*, Nucl. Phys. B **306** (1988) 746;
B. Andersson, G. Gustafson, L. Lonnblad, U. Pettersson, *Coherence Effects in Deep Inelastic Scattering*, Z. Phys. C **43** (1989) 625.
- [8] Z. Nagy, Z. Trocsanyi, *Multi-jet cross sections in deep inelastic scattering at next-to-leading order*, Phys. Rev. Lett. **87** (2001), 082001 [hep-ph/0104315].
- [9] I. Abt *et al.* [H1 Collaboration], Nucl. Instrum. Meth. A **386** (1997) 310;
I. Abt *et al.* [H1 Collaboration], Nucl. Instrum. Meth. A **386** (1997) 348.